

RSC Advances



This is an *Accepted Manuscript*, which has been through the Royal Society of Chemistry peer review process and has been accepted for publication.

Accepted Manuscripts are published online shortly after acceptance, before technical editing, formatting and proof reading. Using this free service, authors can make their results available to the community, in citable form, before we publish the edited article. This *Accepted Manuscript* will be replaced by the edited, formatted and paginated article as soon as this is available.

You can find more information about *Accepted Manuscripts* in the [Information for Authors](#).

Please note that technical editing may introduce minor changes to the text and/or graphics, which may alter content. The journal's standard [Terms & Conditions](#) and the [Ethical guidelines](#) still apply. In no event shall the Royal Society of Chemistry be held responsible for any errors or omissions in this *Accepted Manuscript* or any consequences arising from the use of any information it contains.

Cite this: DOI: 10.1039/c0xx00000x

www.rsc.org/xxxxxx

ARTICLE TYPE

Kinetic investigation of photo-catalytic activity of TiO₂/metal nanocomposite in phenol photo-degradation using Monte Carlo simulation

Hamed Moradmand Jalali*

5

*Department of Physical Chemistry, Faculty of Chemistry, University of Kashan, Kashan, Iran.**Corresponding author. E-mail addresses: Haamedmoradmandjalali@gmail.com. Fax: +98 131 3223372.**Received (in XXX, XXX) XthXXXXXXXXXX 20XX, Accepted Xth XXXXXXXXXXXX 20XX*

DOI: 10.1039/b000000x

10

Kinetic Monte Carlo simulation was applied to study kinetics and photo-catalytic activity mechanism of TiO₂ anatase, P25, Au/TiO₂, Pd/TiO₂ and Au-Pd/TiO₂ applied in photo-degradation of water pollutant including phenol. The reaction kinetic mechanisms of each aforementioned catalytic systems has been obtained. The values of the rate constant for the each step of the reaction mechanisms were gained as adjustable parameters by kinetic Monte Carlo simulation. It was shown the rate constant of formation of electron/hole pairs in metal loaded on titanium dioxide is more than undoped TiO₂ because of electron transmission from titanium dioxide to the metal core. The kinetic study of metal performance in M/TiO₂ nano composite has been demonstrated the rate constant value of electron transfer from TiO₂ to Au is higher than Pd and Au-Pd. In this research the kinetic Monte Carlo simulation results agree qualitatively with the existing experimental data for phenol photo-decomposition.

15

20

1. Introduction

Titanium dioxide has been widely applied in many fields such as photocatalysis,^{1,2} water decontamination,³⁻⁵ air detoxification,^{6,7} dye-sensitized solar cells,^{8,9} and production of hydrogen^{10,11} due to its high stability in UV light and water. Over the last few years the photo-catalytic activity of TiO₂ was successfully enhanced by modification its surface structure, surface properties and composition.¹²⁻¹⁷ In numerous investigations the surface modifying has been performed by loading of metal ions and organic polymers.¹⁸⁻³⁰ Metal nanoparticle (NPs) supported on TiO₂ has been demonstrated to be a promising method to improve the photo-catalytic performance of titanium dioxide. Contact of TiO₂ with metal influences the energetics and the recombination kinetics. On the other hand, the metal-TiO₂ composite nanoparticles facilitates charge separation and charge trapping efficiency of TiO₂ by rectifying the direction of the holes and electrons flow.³¹⁻³³ It has been proven the attachment of the metal nanoparticles can shift the Fermi level of TiO₂, which results in enhanced photo-catalytic reduction activity.^{34,35} The application of metal-titanium dioxide nano composite to purification of water and air has also attracted extensive attention during the recent years. For example, TiO₂-Pt nanotube has been applied for enhanced photo-catalytic degradation of water pollutant by Huan Chen et al.³⁶ Also Au/TiO₂ thin films has demonstrated efficient

photo-catalytic removal of water contaminant containing phenol in sunlight.³⁷ At the recent work photo-decomposition of phenol has been promoted using TiO₂ doped with Au, Pd, and Au-Pd nanoparticles.³⁸

In this research kinetic parameters and the photo-catalytic mechanism of titanium dioxide and modified titanium dioxide was investigated using computational simulation. Kinetic Monte Carlo (kMC) method has been proven a significant level of application as a powerful tool in modelling of various chemical reactions.³⁹⁻⁴³ In the present work an efficient method has been employed for identification and comparison of photo-destruction kinetic mechanisms of phenol over TiO₂ anatase, TiO₂-P25 nano and nano-composite of M/TiO₂ (M= Au, Pd and Au-Pd) using kinetic Monte Carlo simulation. The kinetic mechanisms and the rate determining step of abovementioned photo-catalytic systems were obtained. The rate constant of each step was also determined for each systems by kMC method. The kinetic performance of metal in M/TiO₂ composite was recognized by theoretical kinetic study. Moreover it was gained the concentration curves versus time for photo-oxidation process of phenol by simulation.

2. Kinetic Monte Carlo method

In order to modelling of the experimental data for photocatalytic removal of phenol by different catalyst, we used the kinetic

Monte Carlo simulation developed by Gillespie.⁴⁴ Kinetic simulations were carried out by the help of the Chemical Kinetic Simulator software, version 1.01.⁴⁵ In the algorithm of this simulation the reaction mechanism is considered as a series of several reactions:



The input data for the kinetic simulation are the steps, the rate constants of each step (k_i) and number of molecules (C_i). The algorithm of this modelling is based on the reaction probability density function ($P(\tau, i)$) which is obtained by Master equation:

$$P(\tau, i) = k_i C_i \exp\{-\sum k_i C_i \tau\} \quad (2.2)$$

The $P(\tau, i)$ is two-variable probability density function that can be written as the product of two one-variable probability density functions:

$$P(\tau, i) = P(\tau) \cdot P(i) \quad (2.3)$$

Here $P(\tau)$ is the probability of happening of the next reaction between times $t+\tau$ and $t+\tau+d\tau$, irrespective of which reaction it could be and $P(i)$ shows the probability that the next reaction may be an R_i reaction that occurs at time $t+\tau$.

By the addition theory for probabilities, $P(\tau)$ is obtained by summing of $P(\tau, i)$ over all i -values:

$$P(\tau) = \sum_{i=1}^M P(\tau, i) \quad (2.4)$$

That $P(i)$ is gained by substitution of equation (2.4) in equation (2.3) as:

$$P(i) = P(\tau, i) / \sum_{i=1}^M P(\tau, i) \quad (2.5)$$

These two equations obviously represent the two one-variable density functions in equation (2.3) that give two-variable density function $P(\tau, i)$. By substituting of equation (2.2) in equations (2.4) and (2.5) $P(\tau)$ and $P(i)$ are afforded as:

$$P(\tau) = a \exp(-a\tau) \quad 0 \leq \tau < \infty \quad (2.6)$$

$$P(i) = \frac{a_i}{a} \quad (i = 1, 2, \dots, M) \quad (2.7)$$

Where we have in summary:

$$a_i = k_i C_i \quad (i=1, 2, \dots, M) \quad (2.8)$$

$$a = \sum_{i=1}^M a_i = \sum_{i=1}^M k_i C_i \quad (2.9)$$

In this special case, $P(i)$ is independent of τ . It is also noted that, both of these one-variable density functions are correctly standardized over their respective explanation:

$$\int_0^{\infty} P(\tau) d\tau = \int_0^{\infty} a \exp(-a\tau) d\tau = 1, \quad \sum_{i=1}^M P(i) = \sum_{i=1}^M \frac{a_i}{a} = 1$$

The idea of this simulation method is creating a random value of τ in accord with $P(\tau)$ in equation (2.6), then generate a random integer i according to $P(i)$ in equation (2.7). The result of random pair (τ, i) can be divided according to $P(\tau, i)$.

A random value τ can be generated by clearly drawing a random number r_1 , from the uniform distribution in the unit interval and calculating

$$\tau = \left[\frac{1}{a} \right] \ln \left[\frac{1}{r_1} \right] \quad (2.10)$$

Then, a random integer i may be created by drawing another random number r_2 from the uniform distribution in the unit interval by taking i to be that integer for which,

$$\sum_{v=1}^{i-1} a_v < r_2 a \leq \sum_{v=1}^i a_v \quad (2.11)$$

In this method, two random numbers r_1 and r_2 are created and τ and i are calculated by equation (2.10) and equation (2.11), respectively.

The simulation was extended by constantly selecting at random among the probability weighted steps in the mechanism and updating the reactants and products populations according to stoichiometry of the selected step, system state variables and reaction rates. The final results were obtained as concentration versus time curves. This stochastic numerical simulation has been used to modelling of several chemical reactions.³⁹⁻⁴³ In this project kinetic Monte Carlo simulation has been applied to kinetic study of photo-degradation of phenol by various catalytic system containing TiO₂ anatase, P25 nano and nanocrystalline of M/TiO₂ (M= Au, Pd and Au-Pd).

3. Results and discussion

In this research, it was studied kinetic mechanism of experimental photo-catalytic removal of phenol by a variety of catalytic system containing TiO₂,⁴⁶ P25 nano,³⁸ metal nanoparticles (i.e., Au, Pd, Au-Pd) supported on TiO₂ surface.³⁸ Sobczynski and his coworkers have investigated the photo-degradation of phenol using TiO₂ anatase.⁴⁶ Also the photo-decomposition of phenol has been performed using P25 and TiO₂ doped with Au, Pd and Au-Pd nanoparticles by Ren Su et al.³⁸ The curves of phenol concentration versus time were obtained in the aforementioned works. In the present study the kinetics simulating of the photo-catalytic activity of TiO₂ anatase, P25 nano and M/TiO₂ nano composite were carried out using kinetic Monte Carlo method.

3.1. Kinetic simulation of phenol photo-degradation by TiO₂ and P25

In order to simulation of phenol photo-oxidation by TiO₂ anatase, the input data are temperature (301 K), initial concentration of phenol (5.0×10^{-5} M), initial amount of anatase titanium dioxide (0.05gr),⁴⁶ the steps of mechanism and rate constants of each step. Several mechanisms have been examined for the photo-degradation of phenol by TiO₂ using kinetic Monte Carlo simulation. In the mechanism which has a good fitting with experimental kinetic data, electron/hole pair is formed by irradiation of TiO₂. Subsequently the photo-generated hole combines with hydroxyl ions adsorbed on the surface of TiO₂ results in formation of hydroxyl radicals. This radical is strong oxidant which can participate in the oxidation of phenol on the TiO₂ surface. These steps can be described below:



The snapshots of CKS-Reaction Data Entry windows was presented in Fig.1. The reaction mechanism and rate constants

were put in this windows as shown in Fig.1. The right rate constants were determine by changing rate determining step. Also the values of rate constants were adjusted until a reasonable fitting of the simulated kinetic data with the experimental data was obtained. Fig.2. represents a snapshot of the CKS Reaction Conditions window with initial phenol concentrations, the

temperature, volume and pressure conditions for the phenol photo-degradation reaction. Suitable fitting of this mechanism with the experimental photo-degradation data was demonstrated in different initial concentrations of phenol ($[\text{PhOH}]_0 = 7.5 \times 10^{-5}$, 1.0×10^{-4} , 1.5×10^{-4} , 2.1×10^{-4} M). It is proved that the selected rate constants can be exact by these fittings.

The figure displays three sequential screenshots of the 'Reaction Data Entry' window for the reaction mechanism of phenol photo-degradation by titanium dioxide. Each window is titled 'Reaction Data Entry: phenoluv.rxn' and contains the following information:

- Reaction Step 1 of 3:** Reaction equation: $\text{TiO}_2 \Rightarrow \text{h} + \text{e}$. Form of rate constant: Temperature independent. Form of rate law: Derived from stoichiometry. Forward Rate Constant: 0.28 (l/mole-min) units.
- Reaction Step 2 of 3:** Reaction equation: $\text{h} + \text{OH} \Rightarrow \text{OH}^*$. Form of rate constant: Temperature independent. Form of rate law: Derived from stoichiometry. Forward Rate Constant: 3.15 (l/mole-min) units.
- Reaction Step 3 of 3:** Reaction equation: $\text{OH}^* + \text{PhOH} \Rightarrow \text{H}$. Form of rate constant: Temperature independent. Form of rate law: Derived from stoichiometry. Forward Rate Constant: 3.51 (l/mole-min) units.

Each window includes buttons for 'OK', 'Add Another', 'Delete This', 'Undo', and 'Help'.

Fig.1. snapshots of CKS-Reaction Data Entry windows with reaction mechanism, rate constants for the photo-degradation of phenol by titanium dioxide

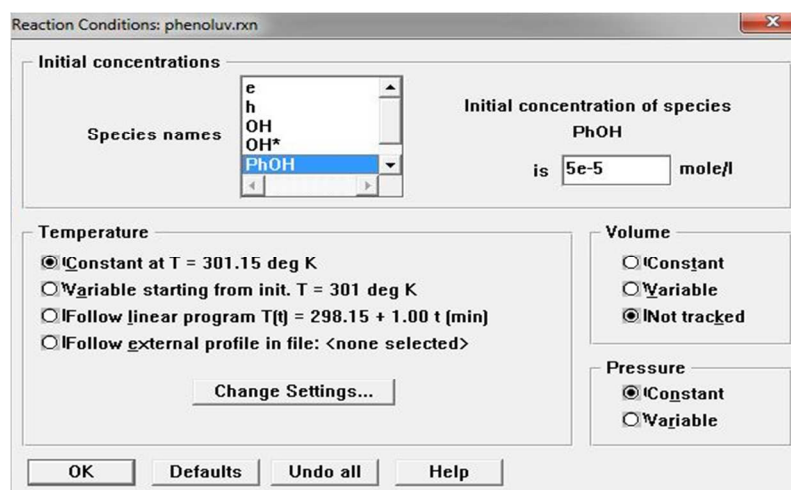


Fig. 2. snapshot of the CKS Reaction Conditions window for the phenol photo-degradation by titanium dioxide

Also the proposed mechanism has been applied to simulation of phenol photo-decomposition by TiO₂-P25 nano (The input data: [PhOH]₀ = 4.00 × 10⁻⁴ M, [P25]₀ = 1 g/L)³⁸ and the value of the rate constants were obtained as adjustable parameter. The rate constants values for photo-degradation of phenol by TiO₂ anatase and P25 nano were listed in Table 1. As seen in the entry 1 of this table, *k*₁, *k*₂ and *k*₃ is constant for five initial concentrations of phenol but there is only the small errors in *k*₂ and *k*₃ for different initial phenol concentration. Furthermore photo-excitation reaction of titanium dioxide (reaction (3.1.1)) is the rate-determining step in phenol photo-destruction by both TiO₂ anatase and P25. Therefore, *k*₁ is more important than other rate constants on the rate of phenol photo-degradation. Moreover *k*₁ of P25 nano is increased rather than TiO₂ anatase while *k*₂ and *k*₃ are constant for the photo-catalytic reaction using both TiO₂ anatase and P25. The difference between *k*₁ of TiO₂ anatase and P25 may be described based on higher surface area of P25 nano. Thus, the enhanced total rate of the photo-induced reaction by P25 is attributed to its greater *k*₁ rather than *k*₁ of TiO₂ anatase.

Table 1. Rate constants of simulated mechanism for photo-degradation of phenol by titanium dioxide

Entry	Catalyst	<i>k</i> ₁ (min ⁻¹)	<i>k</i> ₂ (min ⁻¹)	<i>k</i> ₃ (min ⁻¹)
1 ^a	TiO ₂ anatase	2.80 × 10 ⁻¹	3.15 ± 0.01	3.51 ± 0.1
2 ^b	P25	1.50	3.16	3.56

^a Initial concentration of phenol: 5.0 × 10⁻⁵, 7.5 × 10⁻⁵, 1.0 × 10⁻⁴, 1.5 × 10⁻⁴ and 2.1 × 10⁻⁴ M. Light source: mercury lamp (180W).⁴⁶
^b Irradiation by UV light source (365 nm LED).³⁸

Concentrations of phenol versus time curves have been obtained for different initial concentration of phenol in photo-catalytic reaction by anatase titanium dioxide using kinetic Monte Carlo simulation and results were represented in Fig. 3a. As indicated in this figure, simulated data have good agreement with experimental photo-induced data.⁴⁶ Also there is perfect agreement between kMC simulation and existing experimental data³⁸ as shown in Fig. 3b. These agreements demonstrate that the proposed mechanism can be suitable for study kinetics of photo-degradation of phenol by TiO₂.

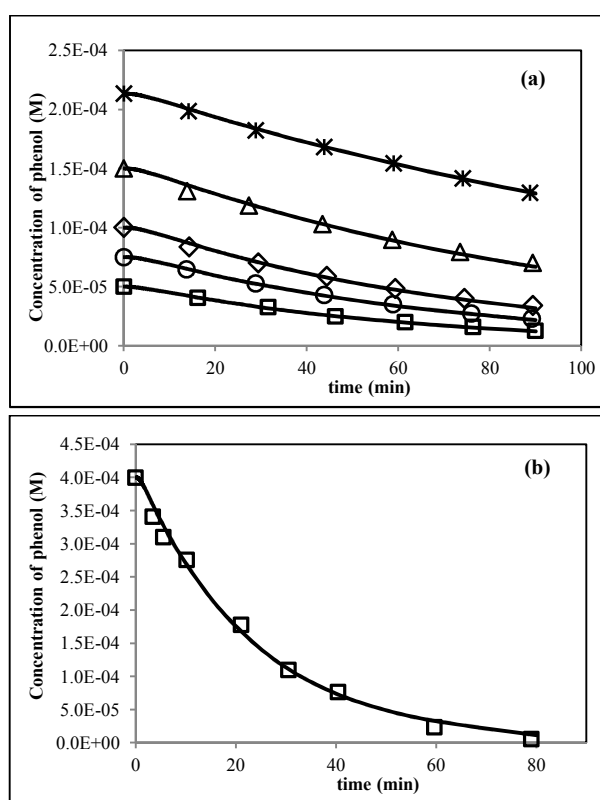
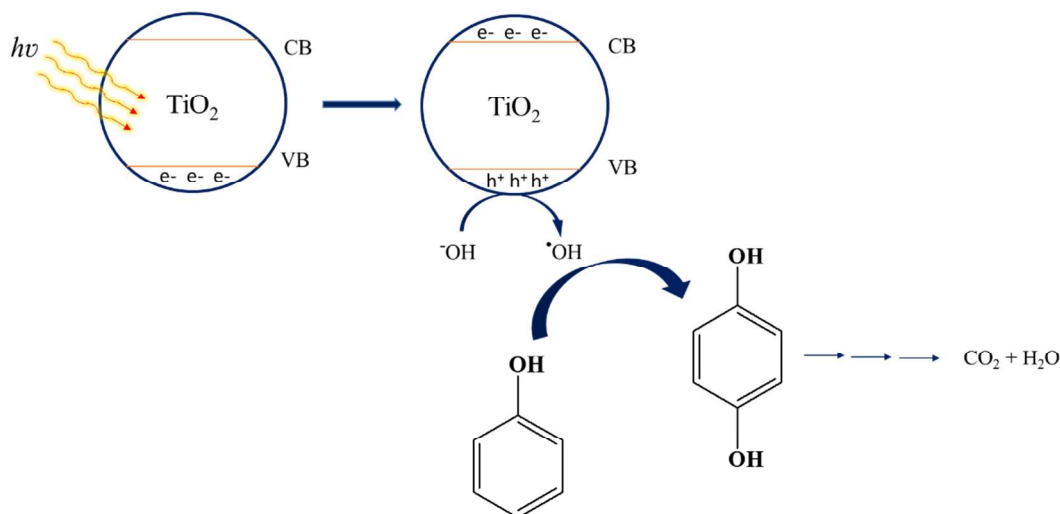


Fig. 3. Kinetics of phenol removal under photo-excitation of (a) TiO₂ anatase (initial concentration of phenol: (□) 5.00 × 10⁻⁵, (○) 7.50 × 10⁻⁵, (◇) 1.00 × 10⁻⁴, (Δ) 1.50 × 10⁻⁴ and (*) 2.1 × 10⁻⁴ M). (b) P25 (initial concentration of phenol: 4.00 × 10⁻⁴ M). Experimental data (open markers) and kMC simulation data (solid line)

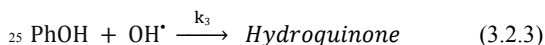
The mechanism of phenol photo-oxidation by TiO₂ has been shown in Scheme 1. Excitation of electrons from the TiO₂ valence band to the conduction band is done by irradiation of titanium dioxide band-gap and the holes are create in the valence band. These photo-holes are reduced by hydroxyl radical on the TiO₂ surface and hydroxyl radical is formed. Subsequently [•]OH initiates phenol oxidation, producing hydroquinone. At the end of this pathway carbon dioxide and water is created by sequential [•]OH attacks to hydroquinone.⁴⁷



Scheme 1. The mechanism of phenol photo-degradation over titanium dioxide

3.2. Simulation of photo-catalytic activity of Pd/TiO₂, Au/TiO₂ and Au-Pd/TiO₂ nanocrystallines in phenol photo-destruction

The kinetic Monte Carlo simulation has been performed to finding the mechanism of photo-catalytic removal of phenol by Pd/TiO₂ nanoparticles. The input experimental data for the simulation are temperature (298.15 K), initial concentration of phenol (4×10^{-4} M), initial concentration of Pd/TiO₂ nanoparticles (1 g/L),³⁸ the steps of proposed mechanism and rate constants of each step. The values of the rate constants were changed until a perfect fitting of the calculated data with the existing experimental results³⁸ was achieved. Various mechanisms have been examined for the catalytic activity of Pd/TiO₂ NPs in phenol photo-oxygenation using kMC simulation. The appropriate mechanism which has been afforded is similar to TiO₂ catalytic mechanism as given below:



The rate constants k_1 , k_2 and k_3 were obtained as adjustable parameters by the simulation and were shown in table 2 (entry 1). The proposed mechanism was also applied to simulation of photo-degradation reaction by Pd-Au/TiO₂ and Au/TiO₂ nano-composites using initial concentration of phenol (4×10^{-4} M) and initial concentration of nano catalyst (1g/L).³⁸ The values of the rate constants of the recent simulations are presented in table 2 (entries 2 and 3). The results of table 2 indicates the rate-determining step is reaction of photo-induced hole with OH⁻ adsorbed on the surface of M/TiO₂ (M= Au, Pd and Au-Pd). The rate constants k_2 and k_3 are almost equal for the photo-decay reaction of phenol by M/TiO₂ nano composites catalyst. Also k_1 of the reaction by Pd/TiO₂ and Pd-Au/TiO₂ are almost constant but enhancement of k_1 is demonstrated in the photo-catalytic

reaction of Au/TiO₂. There are some differences in the kinetic mechanism of phenol photo-decomposition by TiO₂ and M/TiO₂ composites. For example rate determining step is the first step of mechanism in the reaction with TiO₂ and it is the second step in the reaction by M/TiO₂ composites. Furthermore k_1 of M/TiO₂ nano composites are obviously higher than TiO₂ and P25. Therefore the rate of phenol photo-degradation is improved using TiO₂ loaded with Au, Pd and Au-Pd due to increasing of k_1 . The increasing in k_1 of M/TiO₂ nano composites rather than TiO₂ can be described based on immediate transmission of the photo-generated electrons from TiO₂ to the metal nanoparticle and efficient separation of photo-induced electron/hole pairs. Also enhancing k_1 of Au/TiO₂ rather than Pd/TiO₂ can be attributed to the more appropriate electron transfer level of Au combined with TiO₂ than Pd/TiO₂.

Table 2. Rate constants of simulated mechanism for photo-decomposition of phenol by M/TiO₂ nano composite

Entry ^a	Nano Composite	$k_1(\text{min}^{-1})$	$k_2(\text{min}^{-1})$	$k_3(\text{min}^{-1})$
1	Pd/TiO ₂ ^b	1.98×10^1	3.19	4.77
2	Au-Pd/TiO ₂ ^c	2.3×10^1	3.19	4.78
3	Au/TiO ₂ ^d	5.72×10^1	3.22	5.03

^a Irradiation by UV light source (365 nm LED).³⁸

^b Size distribution of Pd/TiO₂ = 2.9 - 3.9 nm.³⁸

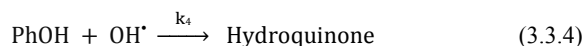
^c Size distribution of Au-Pd/TiO₂ = 2.9 - 4.8 nm.³⁸

^d Size distribution of Au/TiO₂ = 3.0 - 3.7 nm.³⁸

The curves of phenol concentrations versus time have been obtained for the photo catalytic reaction by Pd/TiO₂, Au-Pd/TiO₂ and Au/TiO₂ using kinetic Monte Carlo simulation. The results were illustrated in Fig. 4. As represented in this figure, there is well agreement between simulation data and experimental photo-induced data.³⁸

3.3. The investigation of Au/TiO₂ performance in phenol photo-decomposition

The role of Au/TiO₂ in the photo-degradation reaction was investigated by kinetic Monte Carlo simulation using the available experimental data.³⁷ The study was carried out to simulation of 1% gold loading on the TiO₂ surface (1% Au/TiO₂).³⁷ The input data for the simulation are temperature (298.15 K), initial concentration of phenol (3.19×10⁻⁴ M),³⁷ the steps of suggested mechanism and rate constants of each step. The values of rate constants were adjusted until a reasonable agreement was observed between the simulated and experimental data.³⁷ Different mechanisms have been studied for the photo-decomposition assay by Monte Carlo simulation. The mechanism which has been afforded by kinetic Monte Carlo simulation can be written as:



In the first step of the above mechanism, titanium dioxide is activated at the photo-induced condition and electron/hole pairs are created. The rate constant of this step is k_1 (reaction 3.3.1). Afterward the photo-generated electrons transfer to Au nanoparticle by reaction (3.3.2) with the rate constant k_2 . At the next step the holes move to the nanoTiO₂ surface, participating in an oxidation reaction (3.3.3) and OH^\bullet is formed by the rate constant k_3 . Finally phenol is oxidized by the produced hydroxyl radical (reaction (3.3.4), rate constant = k_4). This proposed mechanism was also used to simulation of phenol photo-degradation by 2% Au/TiO₂.³⁷

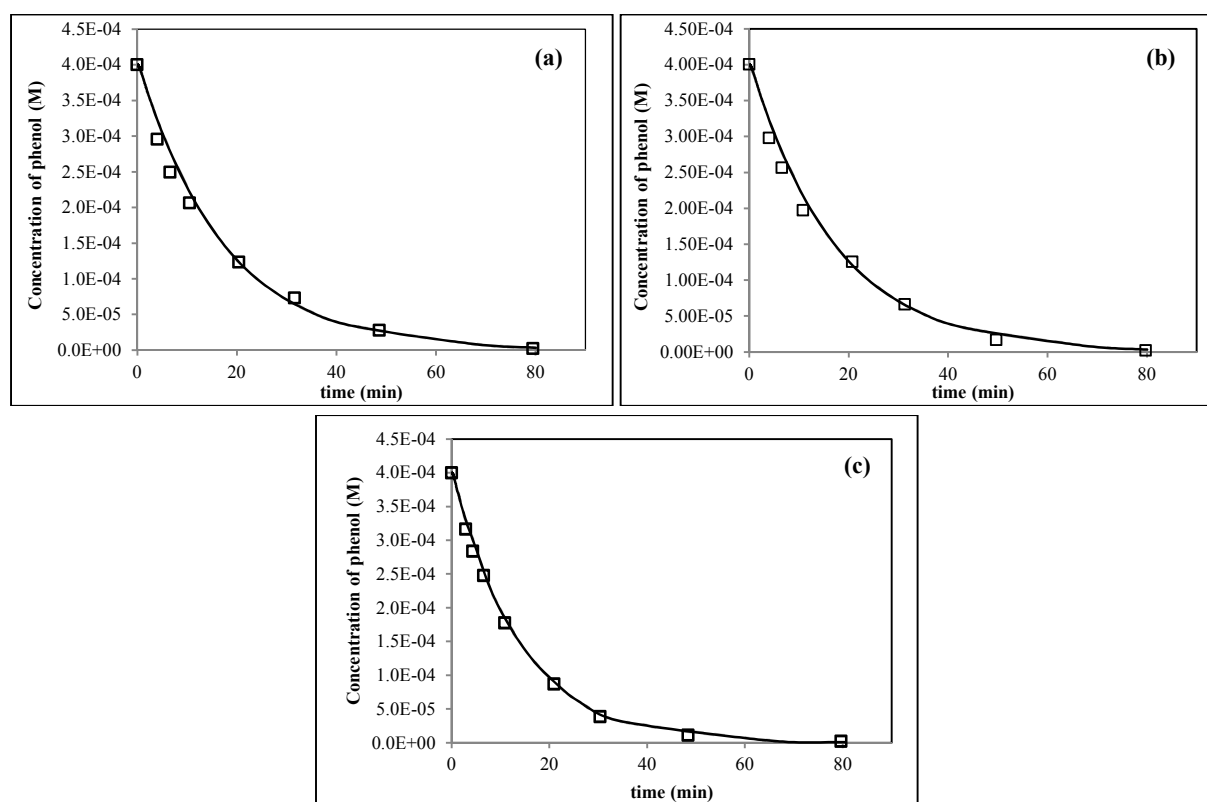


Fig. 4. Kinetic data of phenol photo-degradation by (a) Pd/TiO₂, (b) Au-Pd/TiO₂ and (c) Au/TiO₂ nano composites. Experimental data (open squares) and kMC simulation data (solid line).

The rate constants were obtained as adjustable parameters using kinetic Monte Carlo simulation. The amounts of the rate constants represents the rate-determining step in the aforementioned mechanism is photo-excitation of TiO₂ as shown in Table 3. Furthermore high value of k_2 demonstrates the second step is occurred very fast that it proves immediate transmission of the photo-generated electrons from TiO₂ to gold nanoparticle. Therefor an efficient separation of photo-induced electron/hole pairs is provided and the phenol photo-degradation reaction is accelerated than undoped TiO₂. Also as a result of these simulations k_1 , k_2 , k_3 and k_4 are almost constant for this mechanism using 1% and 2% Au/TiO₂.

Table 3. Kinetic parameters of simulated mechanism for phenol photo-destruction over Au/TiO₂

Entry ^a	Catalytic system	$k_1(\text{min}^{-1})$	$k_2(\text{min}^{-1})$	$k_3(\text{min}^{-1})$	$k_4(\text{min}^{-1})$
1	1% Au/TiO ₂	4.17×10^{-1}	14.33	3.17	5.45
2	2% Au/TiO ₂	4.27×10^{-1}	14.35	3.16	5.42

^a Irradiation source: sunlight. Size distribution of doped catalytic system: 15-20 nm.³⁷

Fig. 5 shows concentration of phenol versus time curves for above-mentioned mechanism obtained by kinetic Monte Carlo simulation. As can be seen, simulation data have appropriate fitting with experimental data.³⁷ According to these results, proposed mechanism will be suitable to study kinetics of photo-catalytic activity of metal/TiO₂ system.

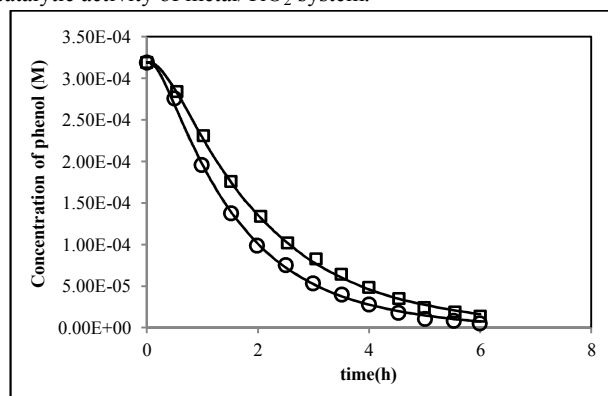
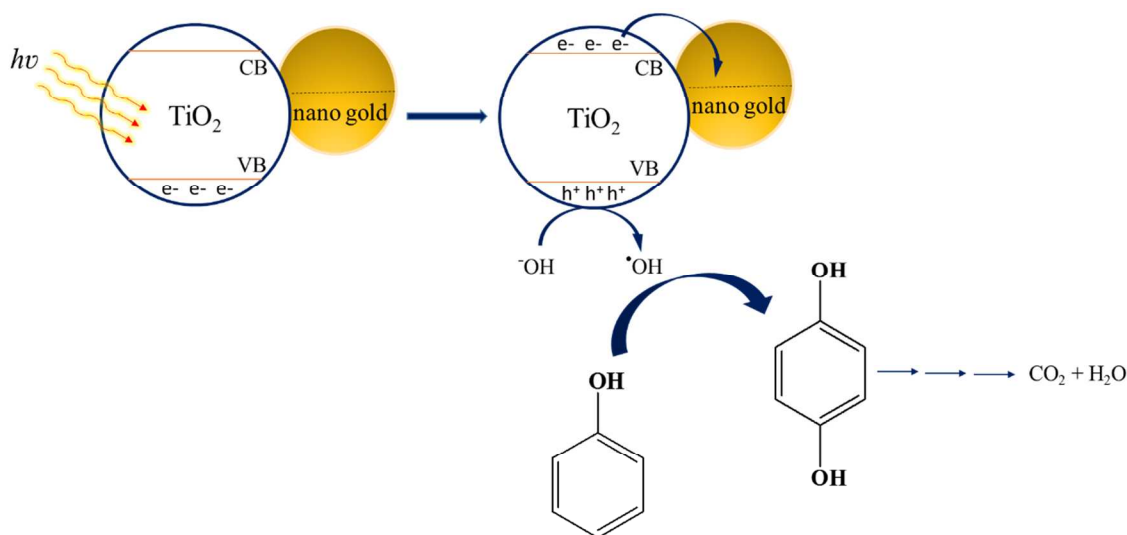


Fig. 5. Kinetic data for photo degradation of phenol by (□) 1% Au/TiO₂, (○) 2% Au/TiO₂. Experimental data (squares and circles mark) and kMC simulation data (solid line).

A probable pathway for the photo-catalytic activity of Au/TiO₂ was illustrated in scheme 2. As shown in this scheme irradiation of TiO₂ band-gap excites electrons to the conduction band and creates holes in the valence band. The photo-generated electrons transfer to the gold core and are stored on it. Subsequently the photo-induced holes are scavenged by OH⁻ adsorbed on the TiO₂ surface, producing [•]OH. Then hydroxyl radical is substituted on the aromatic ring of phenol and hydroquinone is formed. Finally



Scheme 2. The probable mechanism of photo-catalytic activity of Au/TiO₂ in phenol photo-decomposition

4. Conclusions

We used kinetic Monte Carlo simulation as an efficient method to predict and study the kinetics and mechanism of photo-catalytic activity of TiO₂ anatase, P25 and metal nanoparticle loaded on TiO₂ surface in phenol photo-degradation. The kinetic Monte

carbon dioxide and water is created by sequential oxidation of hydroquinone.^{36,48}

This mechanism and pathway can be used to explanation of photo-catalytic performance of other metals in M/TiO₂ systems. For example palladium is also performed to capture of electron in photo condition of Pd/TiO₂ nano-composite. According to the kinetic results which obtained by Monte Carlo simulation, enhanced reaction rate of phenol photo-decomposition by Au/TiO₂ rather than Pd/TiO₂ demonstrates electron migration from conduction band of titanium dioxide to Au is faster than pd. The results are shown in this section, the photo-induced electrons and holes can recombine in the absence of metal. Efficient trapping of photo-generated electrons is occurred by Loading of metal nanoparticle on the TiO₂ surface. The migration of photo-electron to metal core is fast and it is proven using the kinetic results obtained by kMC simulation. These results show that the rate constant of electron transfer step is high value. This process slow down the recombination of electrons and holes and will increase the charge separation efficiency in M/TiO₂ nano composites. Consequently more holes are existing for the photo-oxidation reaction and may effectively improve the catalytic efficiency. Furthermore the differences between the values of k_1 in these studied catalytic systems demonstrate that k_1 depend on the photon flux because the experiments was performed at different photon fluxes.^{37,38,46} The variances between the rate constant of phenol degradation (final step) in the studied systems (in the tables 1, 2 and 3) can be explained by different surface interaction over various catalytic systems. This value is most in Au/TiO₂ nano composite.

Carlo simulated results display qualitative agreement with the phenol photo-decomposition experimental data for the each above catalytic system. Therefore these proposed mechanisms can be appropriate for the kinetic study of photo-catalytic removal of phenol. Our results have shown the rate constant

value of creation of electron/hole pairs is more in M/TiO₂ rather than TiO₂ in terms of electron transfer from titanium dioxide to the metal core. The kinetic study of metal performance in M/TiO₂ nano composite has been proven the electron migration to Au is faster than Pd and Au-Pd.

Acknowledgments

The author is grateful to University of Kashan for supporting this work by Grant No. (256750/I).

References

- 1 S. N. Frank, A. J. Bard, *J. Am. Chem. Soc.*, 1977, 99, 303.
- 2 S. Malato; J. Caceres; A. Aguera, M. Mezcua, D. Hernando; J. Vial, A. R. Fernandez-Alba, *Environ. Sci. Technol.* 2001, 35, 4359.
- 3 A. Fujishima, K. Honda, *Nature*, 1972, 238, 37.
- 4 J. Nowotny, T. Bak, M. K. Nowotny, L. R. Sheppard, *J. Phys. Chem. B*, 2006, 110, 18492.
- 5 J. H. Park, O. O. Park, S. Kim, *Appl. Phys. Lett.*, 2006, 89, 163106.
- 6 C. H. Ao, S. C. Lee, *Chem. Eng. Sci.*, 2005, 60, 103.
- 7 Y. Q. Cao, T. He, Y. M. Chen, Y. A. Cao, *J. Phys. Chem. C*, 2005, 114, 3627.
- 8 B. O. Regan, M. Gratzel, *Nature*, 1991, 353, 737.
- 9 G. K. Mor, K. Shankar, M. Paulose, O. K. Varghese, C. A. Grimes, *Nano Lett.*, 2006, 6, 215.
- 10 S. C. Moon, H. Mametsuka, S. Tabata, E. Suzuki, *Catal. Today*, 2000, 58, 125.
- 11 J. S. Jang, W. Li, S. H. Oh, J. S. Lee, *Chem. Phys. Lett.*, 2006, 425, 278.
- 12 M. Anpo, Y. Ichihashi, M. Takeuchi, H. Yamashita, *Stud. Surf. Sci. Catal.*, 1999, 121, 305.
- 13 M. Anpo, *Catal. Surv. Jpn.*, 1997, 1, 1.
- 14 M. Anpo, Y. Ichihashi, M. Takeuchi, H. Yamashita, *Res. Chem. Intermed.*, 1998, 24, 143.
- 15 M. Anpo, M. Che, *Adv. Catal.*, 1999, 44, 119.
- 16 A. Kudo, M. Sekizawa, *Chem. Commun.*, 2000, 1371.
- 17 K. Sayama, H. Arakawa, *J. Chem. Soc. Faraday. Trans.*, 1997, 93, 1647.
- 18 X.Z. Li, F.B. Li, *Environ. Sci. Technol.*, 2001, 35, 2381.
- 19 V. Subramanian, E. Wolf, P.V. Kamat, *J. Phys. Chem. B*, 2001, 105, 11439.
- 20 F. Boccuzzi, A. Chiorino, M. Manzoli, D. Andreeva, T. Tabakova, L. Ilieva, V. Idakiev, *Catal. Today*, 2002, 75, 169.
- 21 M. Date, Y. Ichihashi, T. Yamashita, A. Chiorino, F. Boccuzzi, M. Haruta, *Catal. Today*, 2002, 75, 51.
- 22 N. Chandrashekhara, P.V. Kamat, *J. Phys. Chem. B*, 2000, 104, 10851.
- 23 M. Valden, X. Lai, D.W. Goodman, *Science*, 1998, 281, 1647.
- 24 D. Andreeva, V. Idakiev, T. Tabakova, L. Ilieva, P. Falaras, A. Bourlinos, A. Travlos, *Catal. Today*, 2002, 72, 51.
- 25 M. Haruta, *Catal. Today*, 1997, 36, 153.
- 26 A. Furube, T. Asahi, H. Yamashita, M. Anpo, *J. Phys. Chem. B*, 1999, 103, 3120.
- 27 A. Furube, T. Asahi, H. Masuhara, H. Yamashita, M. Anpo, *Res. Chem. Intermed.*, 2001, 27, 177.
- 28 A. Furube, T. Asahi, H. Masuhara, H. Yamashita, M. Anpo, *Chem. Phys. Lett.*, 2001, 336, 424.
- 29 A. Furube, T. Asahi, H. Masuhara, H. Yamashita, M. Anpo, *Chem. Lett.* 1997, 735.
- 30 M. Takeuchi, M. Matsuoka, H. Yamashita, M. Anpo, J. *Synchrotron. Radiat.*, 2001, 8, 643.
- 31 M. Jakob, H. Levanon, P. V. Kamat, *Nano Lett.*, 2003, 3, 353.
- 32 T. Hirakawa, P. V. Kamat, *Langmuir*, 2004, 20, 5645.
- 33 T. Hirakawa, P. V. Kamat, *J. Am. Chem. Soc.*, 2005 127, 3928.
- 34 G. R. Bamwenda, S. Tsubota, T. Nakamura, M. Haruta, *J. Photochem. Photobiol. A*, 1995, 89, 177.
- 35 K. Mogyorosi, A. Kmetyko, N. Czirbus, G. Vereb, P. Sipos, A. Dombi, *React. Kinet. Catal. Lett.* 2009, 98, 215.
- 36 H. Chen, S. Chen, X. Quan, H. Yu, H. Zhao, Y. Zhang, *J. Phys. Chem. C*, 2008, 112, 9285.
- 37 R. S. Sonawane, M. K. Dongare, *J. Mol. Catal. A: Chemical*, 2006, 243, 68.
- 38 R. Su, R. Tiruvalam, Q. He, N. Dimitratos, L. Kesavan, C. Hammond, J. A. L. Sanchez, R. Bechstein, C. J. Kiely, G. J. Hutchings, F. Besenbacher, *ACS Nano*, 2012, 6, 6284.
- 39 P. Zarzycki, *J. Coll. Inter. Sci.*, 2007, 315, 54.
- 40 L. Liau., C. Y. Lin, *Colloids and Surfaces A: Physicochem. Eng. Aspects.*, 2011, 388, 70.
- 41 H. M. Jalali, *RSC Adv.*, 2014, 4, 32928.
- 42 H. Bashiri, *Chem. Phys. Lett.*, 2013, 575, 101.
- 43 H. Bashiri, H. Moradmand-Jalali, H. Rasa, *Prog. React. Kinet. Mec.* 2014, 39, 281.
- 44 D. T. Gillespie, *J. Comp. Phys.*; 1976, 2, 403.
- 45 IBM, CSK Chemical Kinetics Simulator 1.01, IBM Almaden Research Center; IBM Corporation 1995.
- 46 A. Sobczynski, L. Duczmal, W. Zmudzinski, *J. Mol. Catal. A: Chemical*, 2004, 213, 225.
- 47 M. Pimentel, N. Oturan, M. Dezotti, M. A. Oturan, *App. Cat. B: Environmental*, 2008, 83, 140.
- 48 P. Amaratunga, M. Lee, J. Kim, D. Lee, *Can. J. Chem.* 2011, 89, 1001.

Graphical Abstract

